INORGANIC CHEMISTRY FRONTIERS

CCS 中国化学会 CHINESE CHEMICAL SOCIETY

ROYAL SOCIETY OF CHEMISTRY

Sheet-Like Silicalite-1 Single Crystals with Embedded Macropores Displaying Superior Catalytic Performance

Journal:	*Inorganic Chemistry Frontiers*
Manuscript ID	QI-RES-08-2023-001712.R1
Article Type:	Research Article
Date Submitted by the Author:	25-Sep-2023
Complete List of Authors:	Zhang, Yanfei; Dalian Maritime University, College of Environmental Science and Engineering Qi, Liang; Dalian Institute of Chemical Physics, Chinese Academy of Sciences; University of Chinese Academy of Sciences Zhang, Xiaomin; State Key Laboratory of Catalysis,Dalian Institute of Chemical Physics, Chinese Academy of Sciences, Jiang, Qike; Chinese Academy of Sciences Dalian Institute of Chemical Physics, Lu, Peng; Qingdao Institute of BioEnergy and Bioprocess Technology Chinese Academy of Sciences Xu, Lei; Dalian Institute of Chemical Physics, Chinese Academy of Sciences, Dalian Institute of Chemical Physics, Chinese Academy of Sciences Bell, Alexis; University of California, Chemical and Biomolecular Engineering

ARTICLE

Sheet-Like Silicalite-1 Single Crystals with Embedded Macropores Displaying Superior Catalytic Performance

Received 00th January 20xx,
Accepted 00th January 20xx

DOI: 10.1039/x0xx00000x

Yanfei Zhang, *[a] Liang Qi, [b] Xiaomin Zhang, [c] Qike Jiang, [d] Peng Lu, [e] Lei Xu, *[c] and Alexis T. Bell[f, g]

Unique sheet-like Silicalite-1 single crystals containing intracrystalline macropores (HMS-Silicalite-1) were prepared by urea-assisted, dry-gel synthesis, which uses mesoporous silica spheres (MSS) as both the silica precursor and the macropore template. Urea was found to inhibit crystal growth in the *b*-axis direction and, therefore, play a pivotal role in the formation of the sheet-like crystals. Zeolite growth occurred via "dissolution-crystallization" transformation of MSS to produce macro/microporous Silicalite-1 crystals. Systematic studies revealed that the urea/SiO_2 and H_2O/SiO_2 ratios affect the morphology of the resulting Silicalite-1 zeolites, and that the thickness of HMS-Silicalite-1 platelets can be tuned between 190 nm and 400 nm. It was also found that the H_2O/SiO_2 and urea/SiO_2 ratios can be modulated to match the "inhibition" and "dissolution-crystallization" processes. HMS-Silicalite-1 was assessed as a catalyst for the Beckmann rearrangement of cyclohexanone oxime to ε-caprolactam and found to exhibit significantly greater resistance to deactivation than conventional Silicalite-1 and hierarchical macro/microporous Silicalite-1. The superior performance of HMS-Silicalite-1 is attributed to the presence of crystals of Silicalite-1 that are thin in the direction of the *b*-axis and contain significant macropores (150 to 400 nm in size). The results of this study offer a novel, yet simple, method for simultaneous control of zeolite crystal aspect ratio and macropore content to produce catalysts that are highly efficient for diffusion-limited reactions involving large reactant molecules.

Introduction

Zeolites are used extensively as catalysts for refining petroleum to transportation fuels and synthesis of chemicals.[1] One of the advantages of zeolites catalysts derives from their micropore structure, which enables them to exhibit shape-selectivity. However, when the size of reactants and products becomes comparable to that of the zeolite micropores, these species encounter diffusional transport limitations that can lead to low utilization of catalytic active sites as well as deactivation due to coke formation as a consequence of pore blockage.[2-4]

Diffusional transport constraints can be overcome by introducing meso- and macro-porosity into the zeolites crystals either during or after their synthesis, and various methods have been considered for introducing meso- and macro-porosity into zeolites.[2, 5-7] These include post-synthetic desilication/dealumination,[8, 9] as well as assembly synthetic method,[10, 11] and hard/soft-template method via hydrothermal or dry-gel conversion (DGC) strategy.[12, 13] Of particular note is the DGC synthetic method which enables the synthesis of zeolites with hierarchical structures.[14, 15] Unlike hydrothermal synthesis, the DGC approach treats the zeolite precursor with water vapor, which helps to form the desired phase with smaller amounts of structure-directing agent, thereby increasing zeolite yield, reducing waste water pollution and even providing unique advantages for the generation meso- and/or macro-porosity.[15-18] Several kinds of hierarchically porous zeolites have been synthesized successfully via DGC method.[19] Zhou et al. have produced agglomerated BEA nano-zeolites with the assistance of organosilanes using an orientated attachment growth route.[20] Tsapatsis et al. have carried out the synthesis of Silicalite-1 zeolite to form nanocrystals of different sizes using three-dimensionally ordered mesoporous (3DOm) carbon templates to confine the growth of zeolite crystals.[21] Su et al. have reported the synthesis of micron-sized BEA zeolite, containing intracrystalline macro-meso-microporosity, utilizing ordered macro-mesoporous carbon as the template in an in situ confined zeolite crystallization strategy.[22]

Previous work on the development of hierarchical zeolites via the DGC method has focused mostly on producing nano-sized assembles but few instances have been reported of its application for producing single crystals. Xiao et al. found that single-crystal zeolite with mesopores exhibits better hydrothermal stability and higher catalytic activity for the condensation of benzaldehyde with glycerol or hydroxyacetophenone and the alkylation of benzene with benzyl alcohol than their nano-sized counterparts.[13] In recent studies, a family of MFI zeolites including Silicalite-1, ZSM-5 and

[a] Green Shipping and Carbon Neutrality Lab, College of Environmental Science and Engineering, Dalian Maritime University, Dalian 116026, China. E-mail: yfzh920@dlmu.edu.cn orcid.org/0009-0003-3812-5642
[b] National Engineering Research Center of Lower-Carbon Catalysis Technology, Dalian National Laboratory for Clean Energy, Dalian Institute of Chemical Physics, Chinese Academy of Sciences, Dalian 116023, China.
[c] Dalian National Laboratory for Clean Energy, Dalian Institute of Chemical Physics, Chinese Academy of Sciences, Dalian 116023, China. E-mail: leixu@dicp.ac.cn orcid.org/0000-0003-4134-3504
[d] Instrumentation and Service Center for Physical Sciences, Westlake University, Hangzhou, 310024, China.
[e] Qingdao Institute of Bioenergy and Bioprocess Technology, Chinese Academy of Sciences, Qingdao 266101, China.
[f] Chemical Sciences Division, Lawrence Berkeley National Laboratory, Berkeley, California 94720, United States.
[g] Department of Chemical and Biomolecular Engineering, University of California, Berkeley, Berkeley, California 94720, United States.
† Electronic Supplementary Information (ESI) available. See DOI: 10.1039/x0xx00000x

TS-1 with large intracrystalline macropores were synthesized by steam-assisted crystallization of mesoporous silica particles.[23-25] Due to enhanced diffusive transport provided by intracrystalline macropores, the catalyst lifetime of ZSM-5 in the methanol-to-olefins reaction was prolonged and the hierarchical TS-1 single crystals exhibited superior catalytic activity for the epoxidation of 2-octene than conventional nano-sized TS-1. Consequently, to achieve improved diffusion transport and good catalytic stability, it is highly desirable to fabricate zeolite crystals which consist of micron-sized particles containing intracrystalline meso-/macro-pores.

Our previous studies have shown that precursors for the DGC method of zeolite synthesis (usually silica or aluminosilicates) can function as both nutrients for zeolite growth and as templates for the generation of secondary pore structures, thereby avoiding the introduction of secondary hard/soft templates. Following this concept, micron-sized MFI-type zeolite single crystals (Silicalite-1 and H-MFI), containing high concentrations of intracrystalline macropores, were synthesized from mesoporous silica spheres (MSS) and mesoporous aluminosilicate spheres (MASS).[26, 27] Different mechanisms of intracrystalline macropore generation were noted. In the case of hierarchical macro/microporous Silicalite-1, intracrystalline macropores were generated via precise control of the rates of the outside-in dissolution of MSS precursors and the crystallization of the zeolite. In the case of hierarchical macro/microprous H-MFI zeolite synthesis, MASS dissolves from the core to the shell due to its Al-rich external surface to provide nutrients for zeolite crystallization, leading to the in-situ formation of intra-crystallite macropores. Thus, the MASS provides a quasi “space-occupying” effect to construct intracrystalline macropores.

Fabrication of sheet-like zeolites with a diffusion path shortened along one axis is another effective strategy for enhancing zeolite mass transfer and enhancing their activity.[28, 29] Specifically, for MFI-type zeolites possessing an anisotropic framework, in which straight channels along b-axis dominate the transportation of guest molecules, shorter b-axis dimensions are favorable for diffusion and conversion of large molecules such as cyclohexanone oxime.[30] Bifunctional, structure-directing agents featuring spaced quaternary ammonium groups and hydrophobic long-chain alkyl or biphenyl tails have been developed for directing the formation of stacked MFI zeolite nanosheets.[31-33] Notably, despite the encouraging achievements in the synthesis of sheet-like zeolites, specially designed and expensive surfactants are usually required. Xiao and co-workers reported a relatively simple hydrothermal synthesis of sheet-like MFI zeolites, including TS-1, Silicalite-1 and H-MFI, by introducing urea.[34, 35] Most recently, Mintova and co-workers have also explored the utility of urea in the synthesis of MFI zeolite nanosheets in a hydrothermal synthesis system and further demonstrated the efficiency of urea in the formation of plate-like crystals.[36] Selective adsorption of urea suppresses crystal growth along b-axis; however, the improvement in diffusional transport was limited due to the relatively larger dimension of the urea crystals (> 100 nm) compared to that of the zeolite nanosheets. To obtain b-axis thickness of 50 nm, high TPAOH/SiO_2 ratio greater than 0.36 was necessary. It is also noted that the role of urea on the growth of zeolite crystals during DGC synthesis has not been reported. Thus, despite considerable progress in modulating the morphology of zeolites and constructing hierarchical porous structure, attempt to obtain single-crystal zeolites possessing both hierarchical pores and a short dimension along one crystal axis remains challenging. Achieving this goal could open up unique opportunities for facilitating diffusion-limited reactions.

Herein, we describe the DGC synthesis of Silicalite-1 single crystals that contain high concentrations of intracrystalline macropores and are thin the direction of the b-axis. To gain insight into the mechanisms of forming intracrystalline macropores and sheet-like zeolite morphology, the crystallization process was investigated via carefully characterizing the morphology properties and phase composition of the materials at different stages of synthesis. Moreover, systematic studies were carried out in which the urea/SiO_2 ratio and the H_2O/SiO_2 ratio in dry-gel precursors were varied in order to control the precursor dissolution and zeolite crystallization processes. The objective was to promote the transformation of MSS to Silicalite-1 zeolites as well as examine the inhibiting effect of urea on the growth of crystals along b-axis. The resulting material combined the advantages of hierarchical zeolites and lamellar structure to enhance diffusional transport. Notably, this approach does not require the use of expensive secondary templates.

The sheet-like macro/microporous Silicalite-1 zeolite prepared in this study was evaluated for its performance as a catalyst for vapor-phase Beckmann rearrangement of cyclohexanone oxime to ε-caprolactam, the monomer for Nylon-6.[37] The reaction for cyclohexanone oxime to ε-caprolactam is

Currently, more than 90% ε-caprolactam is produced via the conventional cyclohexanone route catalyzed by fuming sulfuric acid.[38] Siliceous MFI zeolites (e.g., Silicalite-1) containing silanol nests, or hydrogen-bonded silanol groups, which are mildly acid, have been investigated as promising heterogenous catalysts for the vapor-phase Beckmann rearrangement of cyclohexanone oxime; however, the micropores in Silicalite-1 readily accumulate coke.[39, 40] Previous studies of the Beckmann rearrangement of oxime over Beta zeolite with relatively large pore also supports that this reaction is diffusion-limited.[38, 41, 42] Our work shows that this problem can be alleviated using Silicalite-1 single crystals with high concentrations of intra-crystallite macropores and low dimensions in the direction of the b-axis. These features of the zeolite crystal offer significantly lower diffusional resistance and higher stability to poisoning by coke formation.

Experimental

Materials

Tetrapropylammonium hydroxide (TPAOH, 40 wt%, Runjing Chemical Co.), urea (99 wt%, Tianjin Damao Chemical Reagent Plant), tetraethyl orthosilicate (TEOS, 98%, Tianjin Kemiou Chemical Reagent Co.), ammonium water (25 wt%, based on NH_3, Tianjin Damao Chemical Reagent Plant), ethanol (99.7 wt%, Tianjin Damao Chemical Reagent Plant) and cetyltrimethylammonium bromide (CTAB, 99%, Tianjin Kemiou Chemical Reagent Co.) were used without any further purification.

Synthetic Procedures

Preparation of mesoporous silica spheres. Mesoporous silica spheres (MSS) were prepared in a basic ethanol-water system following a modified Stöber method (Fig. S1).[23, 26, 27] Typically, 0.40 g of CTAB was dissolved in a mixture of ethanol (149.54 g) and distilled water (64.54 g) at room temperature and then, 9.00 g of ammonium hydroxide in water (25 wt%) was added to the solution described above under magnetic stirring. After stirring for an hour, 1.28 g of TEOS was added and the mixture was stirred continuously for 2 h. The white precipitate formed was collected by centrifugation, washed with deionized water, dried at 383 K, and calcined at 823 K for 6 h to remove any CTAB.

Preparation of sheet-like macro/microporous Silicalite-1 zeolite. A series of hierarchical macro/microporous Silicalite-1 crystals with various b-axis dimensions was synthesized by the dry-gel conversion (DGC) method using different amounts of urea and water. Typically, the desired amount of urea was dissolved in a solution of TPAOH and distilled water. Subsequently, 0.30 g of MSS was impregnated with the above solution such that the molar composition of the mixture was 0.17 TPAOH: 3.0 H_2O: 0.5/0.8/1.0 Urea: 1.0 SiO_2. After drying at room temperature for 2-5 h to vaporize excess water, the resulting dry gel composites with varying water amounts and urea amounts were loaded onto a Teflon plate and sealed in a Teflon-lined stainless-steel autoclave containing 10 mL of water at the bottom. This arrangement allowed the dry gel composite to have access to water vapor but not liquid water. Crystallization was conducted at 423 K for 42 h, after which the product was washed with copious amounts of water, dried at 383 K overnight, and calcined at 823 K for 6 h to remove all organic components. For further reference, the hierarchical macro/microporous Silicalite-1 sheets are denoted as HMS-Silicalite-1-X, where HMS stands for hierarchical macro/microporous sheet and X is the molar ratio of urea/SiO_2. To obtain deeper insight into the modulation of crystal morphology synthesis were carried out with varying water and urea contents and the samples were designated as HMS-S1 to HMS-S7. The typical molar compositions of dry gel composites for synthesis are summarized in Table S1. The H_2O/SiO_2 ratio listed in Table S1 and in the Results and Discussion section below is the molar ratio between residual H_2O in dry gel composites and SiO_2. Hierarchical macro/microporous Silicalite-1 crystals were synthesized using a DGC method of the procedure given in Ref.[26]

Characterization of Materials

Powder XRD patterns were recorded using a PANalytical X'Pert PRO X-ray diffractometer equipped with a Cu-Kα radiation source. Relative crystallinity was determined as a function of crystallization time by comparing the integrated area of the diffraction peak area at 2Θ of 7-9° and 23-25° with the maximum value. Scanning electron microscope (SEM) images were recorded with JSM-7800F and TM3030 instruments operating at acceleration voltage of 1 kV and 15 kV, respectively. To obtain information about the morphology of a sample, SEM images of the same region were recorded at different accelerating voltage (JSM-7800F). Transmission electron microscopy (TEM) measurements and selected-area electron diffraction (SAED) were acquired with a Philips-FEI Tecnai F30 electron microscope. N_2 adsorption-desorption isotherms were measure at 77 K with a Micomeritics ASAP 2020 analyzer. Prior to measurement, samples were degassed at 573 K for 5 h. Total surface areas were evaluated by using the Brunauer-Emmett-Teller (BET) equation, whereas total pore volumes were obtained from the adsorbed volume at relative pressure (p/p_0) of 0.99. Micropore surface areas and micropore volumes were calculated by the t-plot method. FT-IR spectra of surface hydroxyl groups were obtained using a Bruker Tensor 27 spectrometer with a resolution of 4 cm^{-1}. Prior to recording IR spectra, samples were pressed into a self-supporting wafer, placed into a quartz cell, and evacuated at 723 K at 10^{-2} Pa, to remove impurities and adsorbed water.

Catalyst Evaluation

Hierarchical macro-/micro-porous Silicalite-1 was evaluated for the vapor-phase Beckmann rearrangement of cyclohexanone oxime (CHO) using procedures described in our previous studies.[27] The reaction was conducted in a fixed-bed reactor (i.d. = 8 mm) at 623 K with a CHO weight hourly space velocity (WHSV, to Silicalite-1 zeolite mass) of 3 h^{-1} at atmospheric pressure. Typically, 0.20 g of HMS-Silicalite-1-X was loaded into the reactor and activated at 723 K for 1 h under flowing nitrogen (20 mL min^{-1}). Subsequently, the reactor was cooled to 623 K. A high-performance liquid chromatography pump (Dalian ELITE Analytical Instruments Co.) was used to supply the CHO-ethanol solution (weight ratio 1:9) at a flow rate of 6 g h^{-1} into a flow of nitrogen (30 mL min^{-1}) maintained at 513 K. The effluent from the reactor was cooled to 273 – 278 K in a glass condenser, and the liquid product was collected at specified time intervals and analyzed by a gas chromatography.

Results and discussion

Morphology and structural features of hierarchical macro/microporous Silicalite-1 sheets

SEM and selected-area electron diffraction (SAED) were used to characterize the structural characteristics and crystallization of HMS-Silicalite-1-1.0. The sheet-like morphology of this sample is clearly evident in the SEM image shown in Figs. 1A and S2A and the XRD pattern seen in the inset of Fig. S2A demonstrates that the crystal has an MFI structure. In agreement with the

ARTICLE

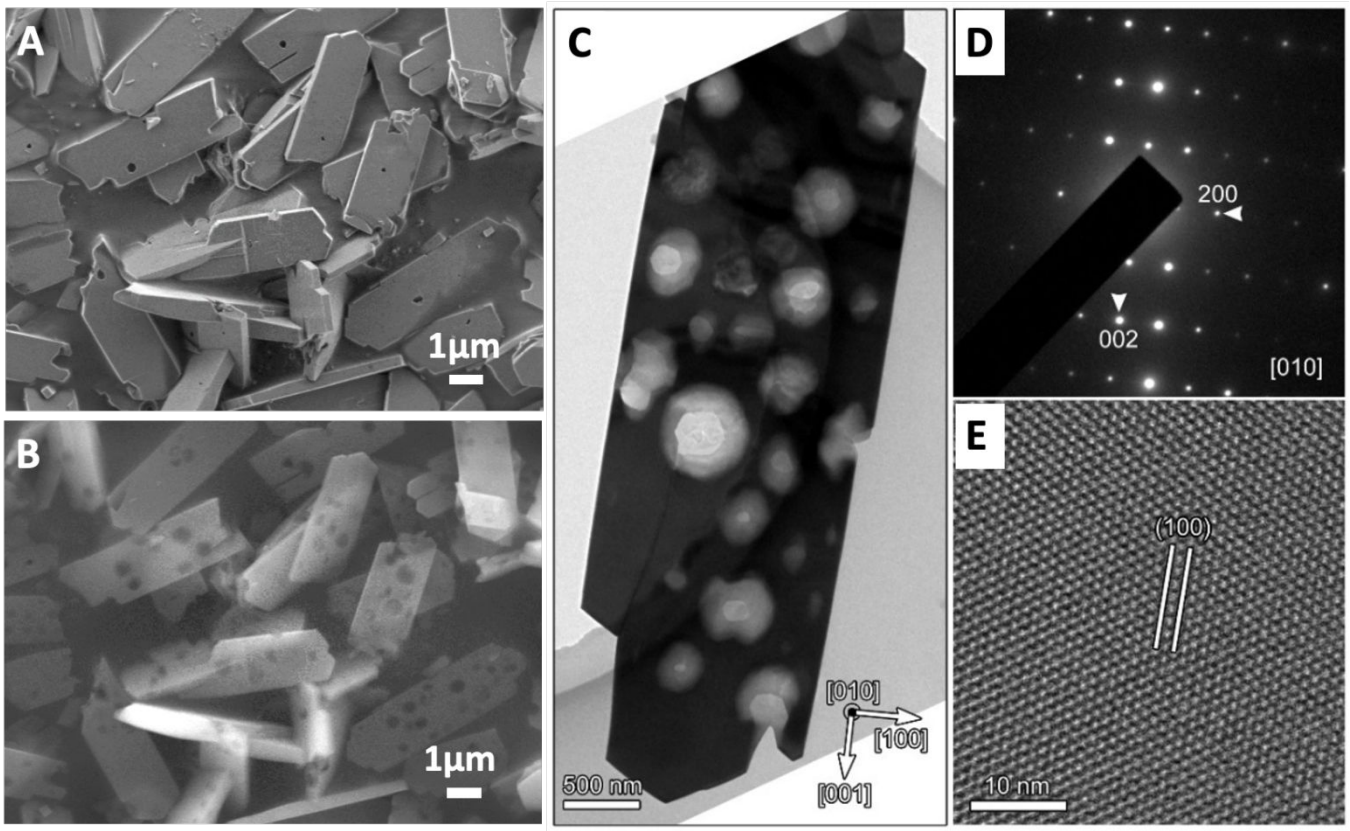

Fig. 1 SEM image of HMS-Silicalite-1-1.0 recorded at low voltage (A) and corresponding high voltage (B). Low magnification TEM image (C), SAED pattern (D) and HRTEM image (E) of HMS-Silicalite-1-1.0.

SEM image recorded at high voltage, the circular grey areas seen in the TEM image at low magnification in Fig. 1C are due to macropores, which suggests that the sheet-like Silicalite-1 contain embedded macropores. The SAED pattern recorded in the direction perpendicular to the flat surface of the crystals is presented in Fig. 1D. Highly distinct and periodically distributed diffraction spots are observed, indicating the single crystalline nature of the HMS-Silicalite-1-1.0 sample. The corresponding high-resolution TEM image (Fig. 1E) shows clear crystal lattice fringes with consistent orientation over the entire imaged region, further confirming the single-crystal character of HMS-Silicalite-1-1.0. Taken together, the TEM and XRD data indicate that the thin edge of the crystals can be indexed as the [010] direction, corresponding to the straight channels parallel to the b-axis, of the MFI zeolite structure.[35, 43]

Interestingly, upon decreasing the SEM accelerating voltage to 1 kV, almost no macropores are observed on the surface of crystals (Figs. 1B and S2B). However, as labelled in the rectangular region in Fig. S2B, a few macropores can be observed in the crystal cross section. This suggests that the macropores in sheet-like crystals of Silicalite-1 are located largely within the interior of the crystals. To support this view, SEM images of the same region of HMS-Silicalite-1-1.0 recorded at 1 kV and 15 kV are presented in Fig. 1. In this case, nearly no macropores are observed in the low-voltage image, whereas abundant macropores, ranging from 150 to 400 nm in diameter, are seen in the image taken at high voltage (Fig. 1B), which further demonstrates that the sheet-like Silicalite-1 crystals contain macropores embedded within zeolite body.

N_2 adsorption-desorption measurements were performed to determine the textural properties of HMS-Silicalite-1-1.0 and the results are presented in Fig. S3 and Table S2. As shown in Fig. S3, HMS-Silicalite-1-1.0 exhibits an obvious adsorption feature for $p/p_0 < 0.01$ due to filling of the micropores. A wide hysteresis loop for $0.4 < p/p_0 < 0.9$ and an enhanced uptake of N_2 are also observed, ascribable to capillary condensation in the mesopores. The detailed textural properties of this sample are summarized in Table S2. Specifically, the BET surface area and total pore volume are 389 m^2/g and 0.188 cm^3/g, respectively. Due to the nano-sized sheet-like structure and the presence of macropores within the crystals of HMS-Silicalite-1-1.0, this material exhibits a somewhat larger external surface area of 106 m^2/g than that of macro-/micro-porous

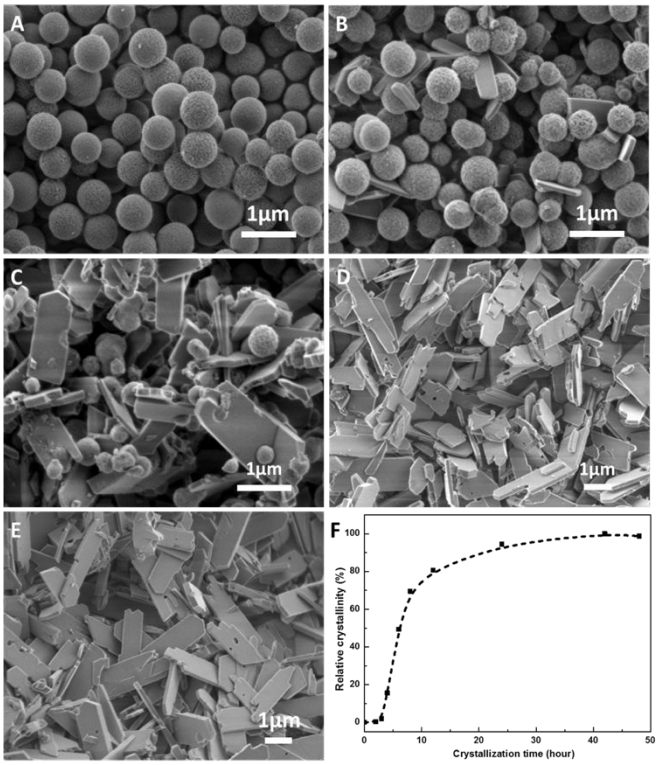

Fig. 2 SEM images of the products synthesized from MSS by urea-assisted dry-gel conversion method for different crystallization time: 2 h (A), 4 h (B), 6 h (C), 12 h (D) and 42 h (E), and variation of relative crystallinity with the extension of crystallization time (F).

HM-Silicalite-1(500) (97 m^2/g) synthesized using the same precursor but without urea.[26]

Systematic study of the synthesis of hierarchical macro/microporous Silicalite-1 sheets

To obtain a deeper understanding of the crystallization process involved in the formation of sheet-like Silicalite-1 embedded with macropores, samples of HMS-Silicalite-1-1.0, prepared with a synthesis composition of 0.17 TPAOH:2.3 H_2O:1.0 Urea:1.0 SiO_2, were characterized by XRD and SEM at various stages of crystallization. As indicated in Fig. S4 (XRD pattern) and Fig. 2A (SEM image), after crystallization for 2 h, the products consist mainly of amorphous silica spheres (500 to 600 nm in diameter). After 3 h, weak diffraction peaks appear characteristic of crystalline MFI (Fig. S4). As the synthesis time is extended to 4 h, the intensity of these peaks increases dramatically and the relative crystallinity (RC) reaches 18 % (Fig. S4 and Fig. 2F).[44] Fig. 2B shows that the MSS precursor had begun to dissolve in the alkaline TPAOH; the surface of spheres is rough and porous (see Fig. S5 for SEM image collected at high resolution), and the diameter of spheres has decreased to 400-500 nm, exhibiting a similar outside-in dissolution behavior of the MSS precursor that was observed in the synthesis of hierarchical macro/microporous Silicalite-1 zeolite without introduction of urea.[26, 45] In contrast to the morphology of the product obtained without urea, sheet-like crystals with thickness of about 60 nm were formed in the initial stage of crystallization (Fig. 2B). By analogy with the work of Xiao and Mintova et al., it is proposed that urea adsorbs on the (010) crystal plane of the crystals during the initial stage of reaction and, therefore, inhibit crystal growth along the b-axis.[35, 36] After crystallization for 6 h, more and more MSS dissolves to provide nutrients for zeolite formation and many more sheet-like crystals embedded with partially dissolved silica spheres appear, suggesting that zeolite forms on the MSS surface (Fig. 2C). This find mirrors the crystallization behaviors of macro/microporous Silicalite-1 around MSS precursors and the transformation of CIT-6 to BEA crystals.[26, 45] When the crystallization time increases to 12 h, the amorphous MSS disappear completely, whereas the zeolite sheets with macropores have grown in directions orthogonal to their b-axis (Figs. 2D and S6A). Consistent with these changes, the RC increases to 80 % and after 42 h of crystallization, the RC reached a maximum of 100 % at which point uniform, sheet-like crystals containing embedded macropores were obtained (Figs. 2E and S6B).

During the crystallization process, it was also observed that the diameter of MSS gradually decreased while the thickness of the crystals increased. This process leads to swallowing of residues of the MSS into the body of the crystals. As evidenced by the SEM image recorded at high voltage (Fig. S6A), macropores were generated in the body of Silicalite-1 crystals as the MSS are completely dissolved and transformed to high-density zeolite crystals. Consequently, it is reasonable to deduce that the macropores are formed from the MSS precursors as a consequence of the velocity difference between the dissolution of MSS and the crystallization of Silicalite-1 zeolite processes. It should be noted that urea decomposition could also contribute to the generation of porosity within Silicalite-1 zeolite. Under alkaline conditions and in the presence of water vapor at high temperature (423 K), urea can undergo hydrolysis to produce ammonia and carbon dioxide ($(NH_2)_2CO + H_2O \rightarrow NH_3 + CO_2$), and the release of these gaseous products could generate defects or meso-/macro-pores in the zeolite crystals.[46] The proposed pore-forming effect is similar to what has been reported during the synthesis of hierarchical SAPO-34 crystals in the presence of $NaHCO_3$.[47] Therefore urea decomposition could contribute to the creations of intra-crystallite pores, mirroring the process that occurs during bread- or popcorn-making. This interpretation is consistent with the type IV N_2 adsorption-desorption isotherm expected for macro-meso-microporous materials.

Based on the observations of the crystallization process presented above, the formation of sheet-like Silicalite-1 with intracrystalline macropores embedded can be ascribed to the synergy between dissolution of the MSS precursors and the simultaneous oriented crystallization of the siliceous species produced by MSS dissolution as well as the formation of gaseous product formed by the decomposition of urea. It is noteworthy that the growth of crystals along b-axis is suppressed significantly by the presence of urea. Scheme 1 illustrates the DGC synthesis process and presents a possible mechanism for the formation of hierarchical macro/microporous Silicalite-1 sheets. As evidenced by the rough outer surface of MSS at initial crystallization stage, amorphous MSS precursors dissolve in an "outside-in" behavior under the effect of alkaline TPAOH to provide nutrients for

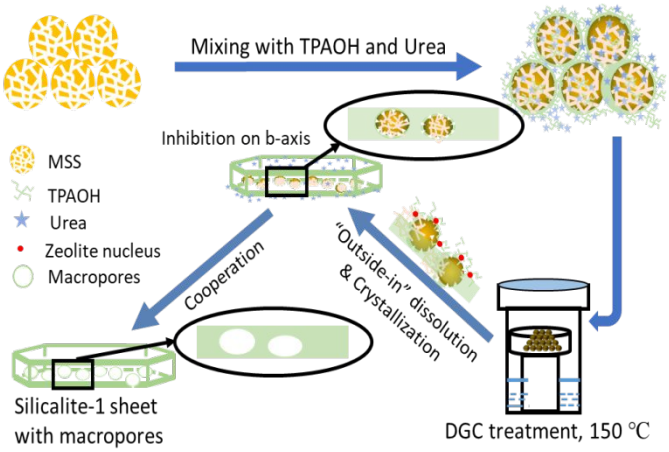

Scheme 1 Schematic illustration of the fabrication process of sheet-like Silicalite-1 embedded with macropores from MSS precursors with the assistance of urea.

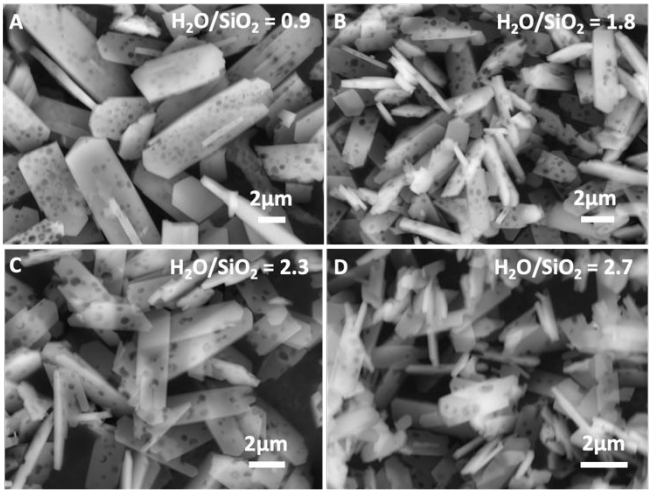

Fig. 3 Effect of H_2O/SiO_2 ratios on the morphology of products at constant urea/SiO_2 ratio of 1.0: (A) H_2O/SiO_2 = 0.9 (HMS-S1), (B) H_2O/SiO_2 = 1.8 (HMS-S2), (C) H_2O/SiO_2 = 2.3 (HMS-Silicalite-1-1.0), and (D) H_2O/SiO_2 = 2.7 (HMS-S3).

zeolite crystallization. Simultaneously, urea adsorbs preferentially on the (010) facets of the growing zeolite crystals thereby inhibiting further growth of the crystals perpendicular to this facet. The net effect is to form sheet-like zeolite crystals during the initial stage of crystallization. Throughout the crystallization process, the MSS precursors dissolve continuously and the dissolved species react to form high-density zeolite crystals. Importantly, under appropriate synthesis conditions, the DGC method provides the spatial proximity of these two processes and Silicalite-1 crystallize on the MSS surface and enables the gradual encapsulation of residual MSS precursors during the crystallization process. Under the synthesis condition employed, the rate of MSS dissolution should be faster than the rate of zeolite crystallization. When the MSS precursors have been consumed completely, the rate of crystallization diminishes, and macropores have been generated in place of MSS precursors in the zeolite crystals. With the cooperation of such dissolution-crystallization process for the transformation of MSS to zeolite crystals and inhibition effect introduced by urea, sheet-like Silicalite-1 crystals containing a high concentration of embedded macropores are formed. We also note that intra-crystallite pore can also form due to urea hydrolysis to produce ammonia and carbon dioxide, which afterward leave crystals, leading to the mesoporosity and possible macroporosity.

Effect of synthesis conditions on the formation of hierarchical macro/microporous Silicalite-1 sheets.

As discussed above, the successful fabrication of sheet-like Silicalite-1 with internal macropores results from the synergy of the dissolution of the MSS precursors, crystallization of Silicalite-1, and urea inhibition of crystal growth along b-axis. Therefore, the dependence of these factors on the formation of HMS-Silicalite-1 crystal was investigated with the aim of understanding which ones modulate the crystal morphology and the formation of macropores. Previous studies have suggested that DGC synthesis is sensitive to the amount of water, since it affects the dissolution of the precursors and nucleation/growth of the zeolites.[48, 49] Water may also affect the inhibition by urea on MFI crystal growth in the direction of the b-axis. For this reason, the effect of water content in the precursor (represented as H_2O/SiO_2 ratio) on the formation of products was investigated first.

For a fixed crystallization temperature and amounts of TPAOH and urea, the H_2O/SiO_2 ratio was increased from 0.9 to 1.8 and then to 2.7, and the resulting products were compared with HMS-Silicalite-1-1.0 produced with an H_2O/SiO_2 ratio of 2.3. The products prepared with different H_2O/SiO_2 ratios were characterized by the XRD peaks associated with MFI zeolite (Fig. S7). The SEM images presented in Fig. 3 show the effects of the H_2O/SiO_2 ratio on the sheet-like morphology. When the H_2O/SiO_2 ratio is reduced to 0.9, crystals with dimensions of 10 μm × 3 μm × 700 nm and high concentrations of macropores are obtained (denoted as HMS-S1, Fig. 3A). The dimension of HMS-S1 along the b-axis (700 nm) is much larger than that for HMS-Silicalite-1-1.0, which suggests that the inhibiting effect of urea on crystal growth of crystals in b-axis is less effective with low water content. Increasing the H_2O/SiO_2 ratio to 1.8 (sample HMS-S2, Fig. 3B), decreases the dimension of the crystals to 4.5 ~ 5 μm and a high concentration of macropores is still observed. Moreover, the b-axis dimension of HMS-S2 decreases to 300 nm, indicating an obvious enhancement in the inhibiting effect of urea on crystal growth in this direction. With a further increase of the H_2O/SiO_2 ratio to 2.3, HMS-Silicalite-1-1.0 produces crystal with the shortest b-axis dimension (ca. 190 nm) and a high concentration of macropores (Fig. 3C). These results suggest that increasing the H_2O/SiO_2 ratio accelerates the rate of MSS dissolution, thereby favoring the nucleation of crystals and gradually reducing the size of the final product. More importantly, the decrease in crystal thickness with increasing H_2O/SiO_2 ratio also implies that a sufficiently high-water content is essential for urea to inhibit the growth of crystals in the b-axis direction. It is notable that further increasing the H_2O/SiO_2 ratio to 2.7 (sample HMS-S3, Fig. 3D) causes a decrease in the crystal dimensions to about 2.0 to 3.5 μm × 1 μm × 190 nm but leads to the near disappearance of macropores. It is hypothesized that too much water enhances

the mobility of MSS and disorganized silica species, which was unfavorable for the orderly growth of Silicalite-1 crystals through incorporating silica spheres and consequently, MSS precursors cannot exhibit their "space-occupying" effect effectively.

The preceding discussion shows that the amount of urea used is one of the critical factors facilitating the formation of a sheet-like morphology and that the water content influences the inhibiting effect of urea in the DGC synthetic approach. It should be noted that the introduction of urea can also lead to changes in alkalinity and thereby affect the dissolution of the MSS precursors, which, in turn, influences the balance of dissolution versus crystallization.[26] As found in the study of urea-assisted morphological engineering of MFI nanosheets, addition of urea slows down the zeolite crystallization kinetics.[36] Therefore, considering that the formation of intra-crystallite macropores is determined by the rates of MSS dissolution and Silicalite-1 crystallization, urea is also expected to affect the formation of macropores. Based on this reasoning, the evolution of crystal morphology with different amounts of urea was further investigated and the results are presented in Figs. 4 and 5. The XRD patterns shown in Figs. 4D and 5D confirm that when the urea/SiO_2 ratio decreases to 0.8 and 0.5, the product synthesized with various amounts of water explored in this study all exhibit strong characteristic peaks of MFI zeolite. Specifically, Figs. 4A-C show the evolution of the zeolite morphology and porosity produced with increasing water content synthesized with a constant urea/SiO_2 ratio of 0.8. As the H_2O/SiO_2 ratio increases from 1.5 to 1.8, the resulting products, HMS-S4 and HMS-Silicalite-1-0.8, exhibit a high concentration of macropores, while the crystal morphology undergoes a transformation from large, thick plate-like crystals to relatively small, thin sheet-like crystals. When the H_2O/SiO_2 ratio is set to 1.5, the thickness of crystals increases to 350-400 nm, suggesting that low water content hinders the inhibiting effect of urea. For a water content of H_2O/SiO_2 = 1.8 (sample HMS-Silicalite-1-0.8, Fig. 4B), sheet-like Silicalite-1 crystals having a minimum thickness (250 nm) and containing a high

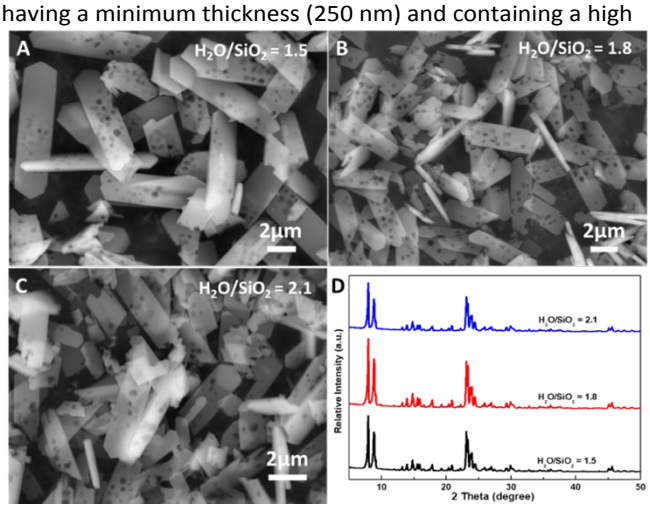

Fig. 4 Effect of H_2O/SiO_2 ratios on the morphology of products at a constant urea/SiO_2 of 0.8: (A) H_2O/SiO_2 = 1.5 (HMS-S4), (B) H_2O/SiO_2 = 1.8 (HMS-Silicalite-1-0.8) and (C) H_2O/SiO_2 = 2.1 (HMS-S5), and (D) the corresponding XRD patterns of samples.

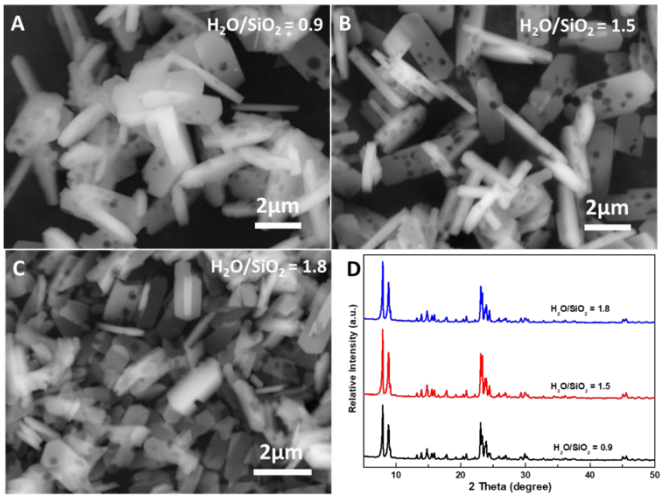

Fig. 5 Effect of H_2O/SiO_2 ratios on the morphology of products at a constant urea/SiO_2 of 0.5: (A) H_2O/SiO_2 = 0.9 (HMS-S6), (B) H_2O/SiO_2 = 1.5 (HMS-Silicalite-1-0.8) and (C) H_2O/SiO_2 = 1.8 (HMS-S7), and (D) the corresponding XRD patterns of products.

concentration of macropores are obtained. Thus, sufficient water not only facilitates urea inhibition of crystal growth along b-axis but also guarantees the proper balance between MSS dissolution and zeolite crystallization, which leads to the formation of a high concentration of macropores. However, further increasing the water content to H_2O/SiO_2 = 2.1 (sample HMS-S5, Fig. 4C), enhances the mobility of silica species dissolved from the MSS precursor and disfavors the ability of MSS to function as macropore-directing template. Consequently, much thinner crystal sheets can be synthesized but with fewer embedded macropores.

As depicted in Fig. 5A-C, when the urea/SiO_2 ratio decreases to 0.5, the zeolite morphology seen with increasing water amount in MSS precursor follows a similar evolution to that obtained at a urea/SiO_2 ratio of 0.8. For an H_2O/SiO_2 ratio of 0.9, HMS-S6 consists of thick crystal sheets with some macropores. Increasing the H_2O/SiO_2 ratio to 1.5 (sample HMS-Silicalite-1-0.8, Fig. 5B) results in an abundance of macropores and a crystallite thickness of ~ 400 nm. Increasing the H_2O/SiO_2 ratio to 1.8, result in the dimensions of the product, HMS-S8, becoming nonuniform and the concentration of macropores becomes negligible.

As demonstrated above, the crystal thickness along the b-axis can be tuned over a wide range by varying the amount of urea introduced. When no urea is added, the crystal thickness along the b-axis rises to 1 μm.[27] For urea/SiO_2 = 0.5, sheet-like crystals with a thickness of about 400 nm are formed. Meanwhile, macropores with diameters between 200 and 400 nm are formed, the size of which is largely consistent with that of macro/microporous Silicalite-1 synthesized previously.[27] When the urea and water content are set to 0.8 and 1.8 respectively, the b-axis dimension of the products decreases to 250 nm. Finally, the thinnest sample HMS-Silicalite-1-1.0 with thickness of 190 nm and rich macropores is obtained for urea/SiO_2 and H_2O/SiO_2 molar ratios of 1.0 and 2.3 respectively. Our studies indicate that the H_2O/SiO_2 ratio should be increased with the urea/SiO2 ratio, a finding not hitherto found for hydrothermal

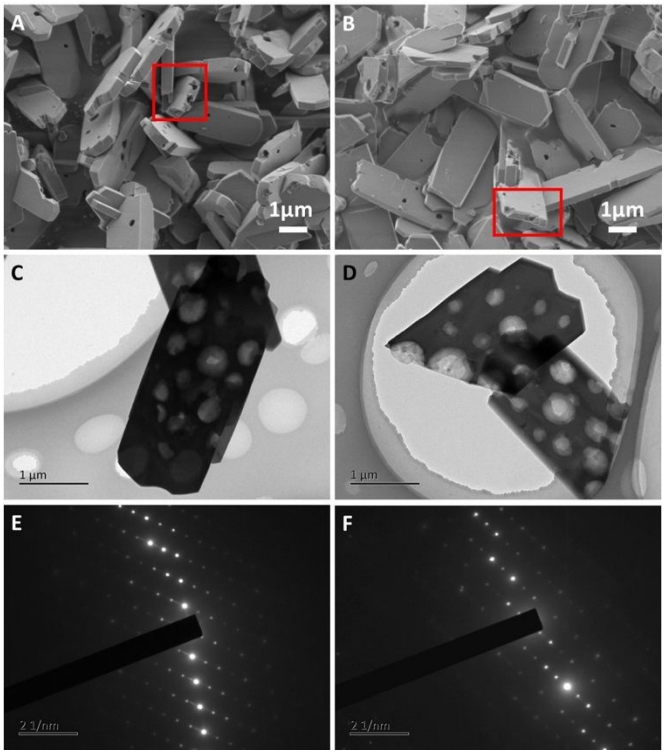

Fig. 6 SEM images (A, B), TEM images (C, D) and SAED patterns (E, F) of samples HMS-Silicalite-1-0.5 and HMS-Silicalite-1-0.8. SEM images were recorded at accelerating voltage of 1 kV.

synthesis of sheet-like MFI.[34,35]

The crystal and textural properties of sheet-like Silicalite-1 synthesized with lower urea addition amounts for samples HMS-Silicalite-1-0.5 and HMS-Silicalite-1-0.8 were further explored systematically by SEM, TEM as well as N_2 physisorption experiments and the results are summarized in Figs. 6, S8 and Table S2. As depicted in the SEM images recorded at low voltage, both Silicalite-1 samples show the near absence macropores at the outer surfaces. But with detailed investigations on the selected areas in Figs. 6A and B (red rectangular areas), macropores could be observed in the cross section of crystals, indicating the presence of macropores in the body of crystals, just like HMS-Silicalite-1-1.0. TEM results (Figs. 6C and D) further demonstrate the sheet-like crystals with rich macropores present. The clear, discrete and periodically distributed spots presented in SAED pattern (Figs. 6E and F) also demonstrate that the two samples HMS-Silicalite-1-0.5 and HMS-Silicalite-1-0.8 are single crystals. Measurements of BET surface area by N_2 adsorption-desorption experiments show that HMS-Silicalite-1-0.5 and HMS-Silicalite-1-0.8 have surface areas of 396-399 m^2/g and large external surface areas of 102-106 m^2/g (Table S2).

Scheme 2 summarizes the conditions necessary for the formation of embedded macropores and attainment of sheet-like morphology. We hypothesize that urea adsorbs on the (010) crystal plane during initial stage of MFI zeolite formation and inhibits its growth along b-axis perpendicular to this crystal plane. Comparative experiments for Silicalite-1 prepared with constant H_2O/SiO_2 molar ratio of 1.8 and increasing urea/SiO_2 molar ratio from 0.5 to 1.0 suggest that the dimension of the crystals along the a-axis increase from ~2 μm to ~5 μm. This study further suggests that urea inhibits the dissolution of the MSS precursor and limits nutrients which subsequently slowing down the zeolite nucleation process resulting in the formation of larger crystals[50].

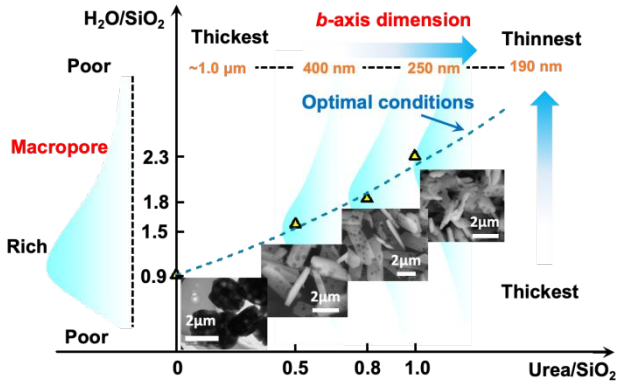

Scheme 2. Illustration for the generation of intracrystalline macropores and sheet-like morphology with reaction conditions.

Catalytic performance in Beckmann rearrangement of cyclohexanone oxime

HMS-Silicalite-1-1.0 was tested for the Beckmann rearrangement of cyclohexanone oxime (CHO) to ε-caprolactam (CP) and compared with the performance of intergrown HM-Silicalite-1 containing only macropores and intrinsic zeolite micropores (Fig. S9). As shown, hierarchical macro/microporous HM-Silicalite-1 prepared using MSS with diameters of 500 nm and 150 nm respectively, which are designated as HM-Silicalite-1(500) and HM-Silicalite-1(150), possess abundant intracrystalline macropores and evidence classic intergrowth morphology. Investigation of HM-Silicalite-1 including HM-Silicalite-1(500) and HM-Silicalite-1(150) with different macropore size has been reported previously, among which the latter material exhibit higher external surface area.[26] Comparison of the catalytic performance of hierarchical macro/microporous sheet-like Silicalite-1 with crystals possessing similar hierarchical macro-/micro-porosity helps to discern the significance of producing nano-sized sheet-like crystals and hierarchical porosity synchronously on improving the catalytic performance of microporous zeolites. Previous studies have suggested that silanol groups are the catalytically active sites in Silicalite-1.[31, 51, 52] Hence, it was of interest to establish the extent to which the DGC method of zeolite synthesis used in this work affected the content and

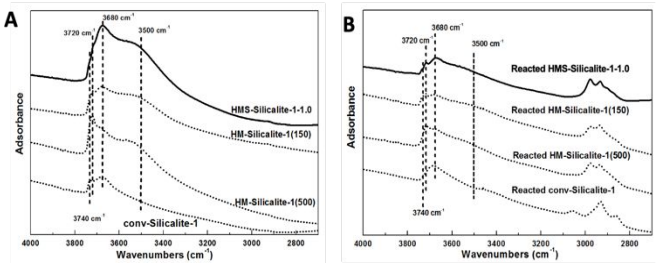

Fig. 7 FTIR spectra of (A) fresh Silicalite-1 samples and (B) Silicalite-1 samples after reaction (conv-Silicalite-1: 6 h, HM-Silicalite-1(500): 57 h, HM-Silicalite-1(150): 57 h, HMS-Silicalite-1-1.0: 57 h).

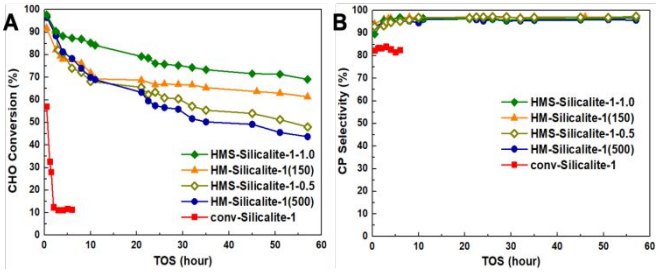

Fig. 8 Evolution of cyclohexanone oxime conversion (A) and ε-caprolactam selectivity (B) with time-on-stream (TOS) over different Silicalite-1 samples during the vapor-phase Beckmann rearrangement reaction. Reaction conditions: 10 wt% CHO in ethanol, WHSV = 3 h^{-1}, 0.2 g catalyst, and temperature = 623 K.

distribution of silanol groups. Fourier transform infrared (FTIR) spectroscopy was used to characterize the distribution of silanol groups in HMS-Silicalite-1-1.0. IR spectra for this product and for HM-Silicalite-1 - HM-Silicalite-1(500) and HM-Silicalite-1(150)), as well as conventional Silicalite-1 are presented in Fig. 7. All four samples exhibit adsorption band at 3740, 3720, 3680 and 3500 cm^{-1} which can be assigned to the terminal silanol groups, asymmetric hydroxyl-bonded silanol groups, vicinal silanol groups, and highly hydrogen-bonding silanol nest-like species respectively.[53] The intensity of all forms of silanol groups in HMS-Silicalite-1-1.0 is significantly higher than for the other three samples, indicating a higher content of silanol groups in this material.

Fig. 8 illustrates the variation in CHO conversion and the selectivity to CP with time-on-stream (TOS) for different forms of Silicalite-1. In sharp contrast to conventional microporous Silicalite-1 (conv-Silicalite-1), sheet-like hierarchical macro/microporous HMS-Silicalite-1-1.0 crystals with a b-axis dimension of about 190 nm exhibits an initial CHO conversion of about 97% as does HM-Silicalite-1(500), and even slightly higher than HM-Silicalite-1(150) (92%); however, all three samples slowly deactivate. However, the CHO conversion on HMS-Silicalite-1-1.0 remains at 85% after 10 h of TOS, while HM-Silicalite-1, which only possess hierarchical macro/micropores, decrease more rapidly to about 70% after the same TOS. As the reaction proceeds, much slower deactivation is observed for all three hierarchical porous catalysts. For the longest TOS (57 h), the CHO conversion over HMS-Silicalite-1-1.0 remains at 69%. The high catalytic stability of HMS-Silicalite-1-1.0 is attributed to its short b-axis dimension and high concentration of macropores, which facilitates diffusional transport of CHO and CP. To further reveal the critical role of the b-axis dimension on the catalytic performance of MFI zeolite, HMS-Silicalite-1-0.5 synthesized with the lowest urea amount and hence larger b-axis dimension of around 400 nm was also evaluated in the Beckmann rearrangement of CHO to CP. As expected, HMS-Silicalite-1-0.5 exhibits around 5% superiority in the catalytic activity after 20 h of TOS compared over that of HM-Silicalite-1(500). However, the evolution of CHO conversion with TOS shown in Fig. 8A, shows that the catalytic activity and stability of HMS-Silicalite-1-0.5 are less attractive compared to HMS-Silicalite-1-1.0. The CHO conversion decreases to about 48% after reacting for 57 h. Consistent with these findings, thermogravimetric analysis (TGA) (Fig. S10) shows that the amount of coke accumulated on HMS-Silicalite-1-1.0 is only 4.1 %, which is somewhat lower than that on HM-Silicalite-1(500) (5.2 %) and HM-Silicalite-1(150) (4.3 %). In previous studies, it has been found that terminal silanol and hydrogen-bonded silanol groups in silanol nests are the active sites for CHO conversion over Silicalite-1. The much higher initial conversion over HMS-Silicalite-1-1.0 and HM-Silicalite-1(500) may be partially ascribed to the much higher concentration of nest-like silanol groups in HMS-Silicalite-1-1.0 and terminal silanol groups in HM-Silicalite-1(500), respectively (see Fig. 8A). After reaction, the intensity of the IR bands ascribed to silanol groups decreased significantly. The results presented above demonstrate that imbedding macropores into the crystal body together with the reduction of MFI zeolite crystal dimension along b-axis effectively inhibits the generation of coke and prolongs catalyst lifetime.

The variation of CPL selectivity with TOS is given in Fig. 8B. It is seen that despite the difference in catalytic stability, the CPL selectivity on the four samples is very similar. During the whole reaction period, the CPL selectivity on all the four samples is about 96 ~97 %.

Conclusions

This work has demonstrated that the dry-gel conversion approach to zeolite synthesis produces hierarchical macro/microporous Silicalite-1 sheets starting from amorphous MSS. The b-axis dimension of the synthesized HMS-Silicalite-1 can be reduced to 190 nm when urea/SiO2 ratio is set to 1.0. Moreover, macropores ranging from 150 nm to 400 nm are observed within the Silicalite-1 sheets. A systematic exploration of the crystallization process of HMS-Silicalite-1-1.0 revealed that the MSS precursors is digested to supply nutrients for the synthesis of Silicalite-1 zeolites following a dissolution-crystallization process. During this process, the MSS precursors also act as transient template for intracrystalline generation of macropores, whereas the urea additive adsorbs on the (010) facet of zeolite crystals and inhibit the growth of crystals perpendicular to this facet, i.e., the b-axis direction. Moreover, the urea additive can also go through hydrolysis decomposition to produce gaseous ammonia and carbon dioxide, which can contribute to the generation of intracrystalline mesopores and macropores. Based on a comprehensive exploration of the critical factors affecting product formation, it is found that the dimension of HMS-Silicalite-1 crystals along b-axis can be tuned from 190 nm to 400 nm. Owing to the high diffusion efficiency of hierarchical porous structure and nanosheet-like morphology, the macro/microporous Silicalite-1 zeolite sheets exhibit a remarkably enhanced catalytic stability for the vapor-phase Beckmann rearrangement of CHO – the CHO conversion can be maintained at 69 % after to 57 h of time on stream.

Author contributions

Y. Z. and L. Qi.: Conceptualization, Writing – original draft, Writing – review & editing. X. Z. and P. L.: Writing – review & editing. Q. J.: Visualization. L. X. and A. T. B.: Supervision, Writing – review & editing.

Conflicts of interest

There are no conflicts to declare.

Acknowledgements

This work was supported by the National Nature Science Foundation of China (No. 22302025) and the Fundamental Research Funds for the Central Universities of Dalian Maritime University in China (No. 3132023161 and No. 3132023520). ATB acknowledges support from the Office of Science, Office of Basic Energy Sciences, of the U.S. Department of Energy (DOE) (No. DE-AC02-05CH11231).

References

1 Bai, P.; Etim, U. J.; Yan, Z.; Mintova, S.; Zhang, Z.; Zhong, Z.; Gao, X., Fluid Catalytic Cracking Technology: Current Status and Recent Discoveries on Catalyst Contamination. *Catal. Rev. Sci. Eng.* 2019, **61,** 333-405.

2 Zhou, J.; Fan, W.; Wang, Y.; Xie, Z., The Essential Mass Transfer Step in Hierarchical/nano Zeolite: Surface Diffusion. *Natl. Sci. Rev.* 2019, **7,** 1630-1632.

3 Li, K.; Valla, J.; Garcia-Martinez, J., Realizing the Commercial Potential of Hierarchical Zeolites: New Opportunities in Catalytic Cracking. *ChemCatChem* 2014, **6,** 46-66.

4 Schwieger, W.; Machoke, A. G.; Weissenberger, T.; Inayat, A.; Selvam, T.; Klumpp, M.; Inayat, A., Hierarchy Concepts: Classification and Preparation Strategies for Zeolite Containing Materials with Hierarchical Porosity. *Chem. Soc. Rev.* 2016, **45,** 3353-3376.

5 Hartmann, M.; Machoke, A. G.; Schwieger, W., Catalytic Test Reactions for the Evaluation of Hierarchical Zeolites. *Chem. Soc. Rev.* 2016, **4,** 3313-3330.

6 Na, K.; Jo, C.; Kim, J.; Cho, K.; Jung, J.; Seo, Y.; Messinger, R. J.; Chmelka, B. F.; Ryoo, R., Directing Zeolite Structures into Hierarchically Nanoporous Architectures. *Science* 2011, **333,** 328-332.

7 Yang, Z.; Guan, Y.; Xu, L.; Zhou, Y.; Fan, X.; Jiao, Y., Tetrapropylammonium Hydroxide Treatment of Aged Dry Gel to Make Hierarchical TS-1 Zeolites for Catalysis. *Cryst. Growth Des.* 2023, **23,** 1775-1785.

8 Groen, J. C.; Moulijn, J. A.; Perez-Ramirez, J., Desilication: on the Controlled Generation of Mesoporosity in MFI Zeolites. *J. Mater. Chem.* 2006, **16,** 2121-2131.

9 Yang, S.; Yu, C.; Yu, L.; Miao, S.; Zou, M.; Jin, C.; Zhang, D.; Xu, L.; Huang, S., Bridging Dealumination and Desilication for the Synthesis of Hierarchical MFI Zeolites. *Angew. Chem. Int. Edit.* 2017, **56,** 12553-12556.

10 Gu, F. N.; Wei, F.; Yang, J. Y.; Lin, N.; Lin, W. G.; Wang, Y.; Zhu, J. H., New Strategy to Synthesis of Hierarchical Mesoporous Zeolites. *Chem. Mater.* 2010, **22,** 2442-2450.

11 Azhati, A.; Xie, S.; Wang, W.; Elzatahry, A. A.; Yan, Y.; Zhou, J.; Al-Dhayan, D.; Zhang, Y.; Tang, Y.; Zhao, D., Ordered, Highly Zeolitized Mesoporous Aluminosilicates Produced by a Gradient Acidic Assembly Growth Strategy in a Mixed Template System. *Chem. Mater.* 2016, **28,** 4859-4866.

12 Chen, H.; Wydra, J.; Zhang, X.; Lee, P.-S.; Wang, Z.; Fan, W.; Tsapatsis, M., Hydrothermal Synthesis of Zeolites with Three-Dimensionally Ordered Mesoporous-Imprinted Structure. *J. Am. Chem. Soc.* 2011, **133,** 12390-12393.

13 Zhu, J.; Zhu, Y.; Zhu, L.; Rigutto, M.; van der Made, A.; Yang, C.; Pan, S.; Wang, L.; Zhu, L.; Jin, Y.; Sun, Q.; Wu, Q.; Meng, X.; Zhang, D.; Han, Y.; Li, J.; Chu, Y.; Zheng, A.; Qiu, S.; Zheng, X.; Xiao, F. S., Highly Mesoporous Single-Crystalline Zeolite Beta Synthesized Using a Nonsurfactant Cationic Polymer as a Dual-Function Template. *J. Am. Chem. Soc.* 2014, **136,** 2503-2510.

14 Ge, T. G.; Hua, Z.; He, X. Y.; Lv, J.; Chen, H. R.; Zhang, L. X.; Yao, H. L.; Liu, Z. W.; Lin, C. C.; Shi, J. L., On the Mesoporogen-Free Synthesis of Single-Crystalline Hierarchically Structured ZSM-5 Zeolites in a Quasi-Solid-State System. *Chem.– Eur. J.* 2016, **22,** 7895-7905.

15 Wang, N.; Qian, W.; Shen, K.; Su, C.; Wei, F., Bayberry-like ZnO/MFI Zeolite as High Performance Methanol-to-Aromatics Catalyst. *Chem. Commun.* 2016, **52,** 2011-2014.

16 Zheng, J.; Jin, D.; Liu, Z.; Zhu, K.; Zhou, X.; Yuan, W., Synthesis of Nanosized SAPO-34 via an Azeotrope Evaporation and Dry Gel Conversion Route and Its Catalytic Performance in Chloromethane Conversion. *Ind. Eng. Chem. Res.* 2018, **57,** 548-558.

17 Askari, S.; Sedighi, Z.; Halladj, R., Rapid Synthesis of SAPO-34 Nanocatalyst by Dry Gel Conversion Method Templated with Morphline: Investigating the Effects of Experimental Parameters. *Microporous Mesoporous Mater.* 2014, **197,** 229-236.

18 Zhang, L.; Bates, J.; Chen, D.; Nie, H.-Y.; Huang, Y., Investigations of Formation of Molecular Sieve SAPO-34. *J. Phys. Chem. C* 2011, **115,** 22309-22319.

19 PrasadáRao, P. H., Dry-Gel Conversion Technique for Synthesis of Zeolite BEA. *Chem. Commun.* 1996, **12,** 1441-1442.

20 Chen, J.; Hua, W.; Xiao, Y.; Huo, Q.; Zhu, K.; Zhou, X., Tailoring the Structure of Hierarchically Porous Zeolite Beta through Modified Orientated Attachment Growth in a Dry Gel System. *Chem.– Eur. J.* 2014, **20,** 14744-14755.

21 Fan, W.; Snyder, M. A.; Kumar, S.; Lee, P.-S.; Yoo, W. C.; McCormick, A. V.; Lee Penn, R.; Stein, A.; Tsapatsis, M., Hierarchical Nanofabrication of Microporous Crystals with Ordered Mesoporosity. *Nat. Mater.* 2008, **7,** 984-991.

22 Sun, M. H.; Chen, L. H.; Yu, S.; Li, Y.; Zhou, X. G.; Hu, Z. Y.; Sun, Y. H.; Xu, Y.; Su, B. L., Micron-Sized Zeolite Beta Single Crystals Featuring Intracrystal Interconnected Ordered Macro-Meso-Microporosity Displaying Superior Catalytic Performance. *Angew. Chem. Int. Ed.* 2020, **132,** 19750-19759.

23 Machoke, A. G.; Beltrán, A. M.; Inayat, A.; Winter, B.; Weissenberger, T.; Kruse, N.; Güttel, R.; Spiecker, E.; Schwieger, W., Micro/Macroporous System: MFI-Type Zeolite Crystals with Embedded Macropores. *Adv. Mater.* 2015, **27,** 1066-1070.

24 Weissenberger, T.; Reiprich, B.; Machoke, A. G.; Klühspies, K.; Bauer, J.; Dotzel, R.; Casci, J. L.; Schwieger, W., Hierarchical MFI Type Zeolites with Intracrystalline Macropores: The Effect of the Macropore Size on the Deactivation Behaviour in the MTO Reaction. *Catal. Sci. Technol.* 2019, **9,** 3259-3269.

25 Weissenberger, T.; Leonhardt, R.; Zubiri, B. A.; Pitínová-Štekrová, M.; Sheppard, T. L.; Reiprich, B.; Bauer, J.; Dotzel, R.; Kahnt, M.; Schropp, A., Synthesis and Characterisation of Hierarchically Structured Titanium Silicalite-1 Zeolites with Large Intracrystalline Macropores. *Chem.–A Eur. J.* 2019, **25,** 14430-14440.

26 Zhang, Y.; Xu, L.; Zhang, J.; Li, P.; Yuan, Y.; Guo, H.; Zhang, X.; Xu, L., Insight into the Dissolution–Crystallization Strategy towards Macro/Meso/Microporous Silicalite-1 Zeolites and

Their Performance in the Beckmann Rearrangement of Cyclohexanone Oxime. *Catal. Sci. Technol.* 2018, **8,** 4526-4536.

27 Zhang, Y.; Lu, P.; Yuan, Y.; Xu, L.; Guo, H.; Zhang, X.; Xu, L., One Pot Synthesis of Hierarchically Macro/Microporous ZSM-5 Single Crystals. *CrystEngComm* 2017, **19,** 4713-4719.

28 Prech, J.; Pizarro, P.; Serrano, D. P.; Cejka, J., From 3D to 2D Zeolite Catalytic Materials. *Chem. Soc. Rev.* 2018, **47,** 8263-8306.

29 Garcia-Martinez, J.; Xiao, C.; Cychosz, K. A.; Li, K.; Wan, W.; Zou, X.; Thommes, M., Evidence of Intracrystalline Mesostructured Porosity in Zeolites by Advanced Gas Sorption, Electron Tomography and Rotation Electron Diffraction. *ChemCatChem* 2014, **6,** 3110-3115.

30 Kim, J.; Park, W.; Ryoo, R., Surfactant-Directed Zeolite Nanosheets: A High-Performance Catalyst for Gas-Phase Beckmann Rearrangement. *ACS Catal.* 2011, **1,** 337-341.

31 Chang, A.; Hsiao, H.-M.; Chen, T.-H.; Chu, M.-W.; Yang, C.-M., Hierarchical Silicalite-1 Octahedra Comprising Highly-Branched Orthogonally-Stacked Nanoplates as Efficient Catalysts for Vapor-Phase Beckmann Rearrangement. *Chem. Commun.* 2016, **52,** 11939-11942.

32 Choi, M.; Na, K.; Kim, J.; Sakamoto, Y.; Terasaki, O.; Ryoo, R., Stable Single-Unit-Cell Nanosheets of Zeolite MFI as Active and Long-Lived Catalysts. *Nature* 2009, **461,** 246-249.

33 Xu, D.; Ma, Y.; Jing, Z.; Han, L.; Singh, B.; Feng, J.; Shen, X.; Cao, F.; Oleynikov, P.; Sun, H.; Terasaki, O.; Che, S., π-π Interaction of Aromatic Groups in Amphiphilic Molecules Directing for Single-Crystalline Mesostructured Zeolite Nanosheets. *Nat. Commun.* 2014, **5,** 4262-4270.

34 Liu, Y.; Zhou, X.; Pang, X.; Jin, Y.; Meng, X.; Zheng, X.; Gao, X.; Xiao, F.-S., Improved para-Xylene Selectivity in meta-Xylene Isomerization Over ZSM-5 Crystals with Relatively Long b-Axis Length. *ChemCatChem* 2013, **5,** 1517-1523.

35 Shan, Z.; Wang, H.; Meng, X.; Liu, S.; Wang, L.; Wang, C.; Li, F.; Lewis, J. P.; Xiao, F.-S., Designed Synthesis of TS-1 Crystals with Controllable b-Oriented Length. *Chem. Commun.* 2011, **47,** 1048-1050.

36 Yue, Q.; Liu, C.; Zhao, H.; Liu, H.; Ruterana, P.; Zhao, J.; Qin, Z.; Mintova, S., Urea-Assisted Morphological Engineering of MFI Nanosheets with Tunable b-Thickness. *Nano Res.* 2023, DOI: 10.1007/s12274-023-5749-0.

37 Zhang, P.; Yi, X.; Xia, C.; Peng, X.; Zhang, S.; Li, C.; Zheng, A.; Zhang, X.; Luo, Y.; Cui, L., Rational Construction of Multiple Hollow Silicalite-1 Zeolite with Enhanced Quasi Acidity for Robust Vapor-Phase Beckmann Rearrangement. *Nano Res.* 2023, **16,** 7958-7966.

38 Kaur, K.; Srivastava, S., Beckmann Rearrangement Catalysis: A Review of Recent Advances. *New J. Chem.* 2020, **44,** 18530-18572.

39 Yin, C.; He, J.; Liu, S., Synthesis of Mesoporous Silicalite-1 Zeolite for the Vapor Phase Beckmann Rearrangement of Cyclohexanone Oxime. *Microporous Mesoporous Mater.* 2020, **307,** 110517-110522.

40 Ge, C.; Sun, X.; Lian, D.; Li, Z.; Wu, J., Controllable Synthesis and Structure-Performance Relationship of Silicalite-1 Nanosheets in Vapor Phase Beckmann Rearrangement of Cyclohexanone Oxime. *Catal. Lett.* 2021, **151,** 1488-1498.

41 Dai, L.-X.; Hayasaka, R.; Iwaki, Y.; Koyano, K. A.; Tatsumi, T., Vapour phase Beckmann rearrangement of cyclohexanone oxime catalysed by Hβ zeolite. *Chem. Commun.* **1996,** 9, 1071-1072.

42 Linares, M.; Vargas, C.; García, A.; Ochoa-Hernández, C.; Čejka, J.; Garcia-Munoz, R.; Serrano, D., Effect of hierarchical porosity in Beta zeolites on the Beckmann rearrangement of oximes. *Catal. Sci. Technol.* **2017,** *7*, 181-190.

43 Cundy, C. S.; Cox, P. A., The Hydrothermal Synthesis of Zeolites: History and Development from the Earliest Days to the Present time. *Chem. Rev.* 2003, **103,** 663-701.

44 Sun, M.-H.; Chen, L.-H.; Li, X.-Y.; Yang, Y.; Ouyang, Y.-T.; Geng, W.; Li, Y.; Yang, X.-Y.; Su, B.-L., A Comparative Study of Hierarchically Micro-Meso-Macroporous Solid-Acid Catalysts Constructed by Zeolites Nanocrystals Synthesized via a Quasi-Solid-State Crystallization Process. *Microporous Mesoporous Mater.* 2013, **182,** 122-135.

45 Morgado Prates, A. R.; Pagis, C.; Meunier, F. C.; Burel, L.; Epicier, T.; Roiban, L.; Koneti, S.; Bats, N.; Farrusseng, D.; Tuel, A., Hollow Beta Zeolite Single Crystals for the Design of Selective Catalysts. *Cryst. Growth Des.* 2018, **18,** 592-596.

46 Khan, Z.; Rafiquee, M.; Niaz, M. A.; Khan, A. A., Kinetics and Mechanism of Alkaline Hydrolysis of Urea and Sodium Cyanate. *Indian J. Chem.,* 1996, **35A,** 1116-1119.

47 He, Y.-R.; Zhu, Y.-L.; Duan, Y.; Zhang, M.; Jiang, J., Green Route To Grow Hierarchical SAPO-34 Crystal with Excellent Catalytic Performance in Methanol to Olefin Reaction. *Cryst. Growth Des.* 2020*,* **20,** 17-23.

48 Niphadkar, P. S.; Kotwal, M. S.; Deshpande, S. S.; Bokade, V. V.; Joshi, P. N., Tin-silicalite-1: Synthesis by Dry Gel Conversion, Characterization and Catalytic Performance in Phenol Hydroxylation Reaction. *Mater. Chem. Phys.* 2009, **114,** 344-349.

49 Saha, S. K.; Waghmode, S. B.; Maekawa, H.; Kawase, R.; Komura, K.; Kubota, Y.; Sugi, Y., Magnesioaluminophosphate Molecular Sieves with ATS Topology: Synthesis by Dry-Gel Conversion Method and Catalytic Properties in the Isopropylation of Biphenyl. *Microporous Mesoporous Mater.* 2005, **81,** 277-287.

50 Camblor, M.; Mifsud, A.; Pérez-Pariente, J., Influence of the Synthesis Conditions on the Crystallization of Zeolite Beta. *Zeolites* 1991, **11,** 792-797.

51 Flego, C.; Dalloro, L., Beckmann Rearrangement of Cyclohexanone Oxime over Silicalite-1: An FT-IR Spectroscopic Study. *Microporous Mesoporous Mater.* 2003, **60,** 263-271.

52 Marthala, V. R. R.; Frey, J.; Hunger, M., Accessibility and Interaction of Surface OH Groups in Microporous and Mesoporous Catalysts Applied for Vapor-Phase Beckmann Rearrangement of Oximes. *Catal. Lett.* 2010, **135,** 91-97.

53 Qi, L.; Zhang, Y.; Conrad, M. A.; Russell, C. K.; Miller, J.; Bell, A. T., Ethanol Conversion to Butadiene over Isolated Zinc and Yttrium Sites Grafted onto Dealuminated Beta Zeolite. *J. Am. Chem. Soc.* 2020, **142,** 14674-14687.